Defect-Enhanced Visible Electroluminescence of Multi-Energy Silicon-Implanted Silicon Dioxide Film

Chun-Jung Lin and Gong-Ru Lin, *Senior Member, IEEE*

***Abstract*—White-light and blue–green electroluminescence (EL) of a multirecipe Si-ion-implanted SiO_2 (SiO_2:Si^+) film on Si substrate are demonstrated. The blue–green photoluminescence (PL) is enhanced by the reaction of $O_3 \equiv$ Si-O-Si $\equiv O_3 \rightarrow O_3 \equiv$ Si-Si $\equiv O_3 + O_{\text{interstitial}}$ during Si implantation. After annealing at 1100 °C for 180 min, the luminescence at both 415 and 455 nm is markedly enhanced by the complete activation of radiative defects, such as weak oxygen bonds, neutral oxygen vacancies (NOVs), and the precursors of nanocrystallite Si (E'_δ centers). Absorption spectroscopy and electron paramagnetic resonance confirm the existence of NOVs and E'_δ centers. The slowly rising E'_δ-related PL intensity reveals that the formation of nanocrystallite Si (nc-Si) requires longer annealing times and suggests that the activation energy for diffusion of excess Si atoms is higher than that of other defects in ion implanted SiO_2. The EL from the Ag–SiO_2:Si^+/n-Si–Ag metal–oxide–semiconductor diode changes from deep blue to green as the driving current increase from 0.28 to 3 A. The maximum white-light luminescent power is up to 120 nW at a bias current of 1.25 A.**

***Index Terms*—Electroluminescence (EL), MOS diode, photoluminescence (PL), Si-ion implantation, Si-rich silicon dioxide.**

I. Introduction

SILICON-RICH SiO_2 materials can be synthesized by electron-beam evaporation [1], RF-magnetron sputtering, Si-ion implantation [2], and plasma-enhanced chemical vapor deposition (PECVD) [3].. Previously, porous Si [4], PECVD-grown Si-rich SiO_2, amorphous Si:H:O, and Si-implanted SiO_2 (SiO_2:Si^+) have been shown to exhibit photoluminescence (PL) and electroluminescence (EL) spreading from blue–green to the near-infrared region (340–800 nm) [1], [5]–[9]. Particularly, the structural defects in the silicon-rich SiO_2 responsible for visible PL at 400–500 nm have caused great interest [10]. Silicon implantation usually introduces versatile defects in SiO_2 [11], for example, the neutral oxygen vacancy (NOV) and the nonbridging oxygen hole center (NBOHC) [6], [12], [13]. Some of the radiative defects such as NOV and NBOHC can be activated via appropriate annealing processes. The contribution of NOV defects to the PL at 450–470 nm has been verified in previous reports [14]–[16], whereas the nanocrystallite Si (nc-Si) embedded in the annealed SiO_2:Si^+ matrix contributes to the emission at longer wavelengths [11]. Although two contradictory PL mechanisms exist, most studies focus on the nc-Si-correlated PL characteristics, while few studies have investigated the defect-induced blue–green PL. In this study, the luminescent centers in SiO_2:Si^+ before and after thermal annealing are characterized by absorption spectroscopy and electron paramagnetic resonance (EPR). The defect-enhanced EL from an SiO_2:Si^+-based MOS diode and its corresponding mechanisms are reviewed.

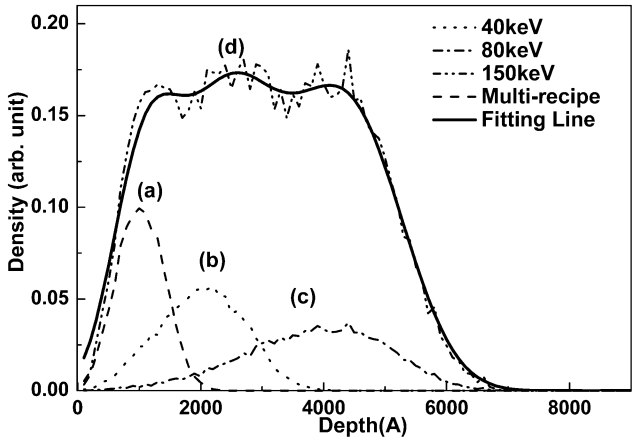

Fig. 1. TRIM calculations for Si-ion implantation into 500-nm-thick SiO_2 film with (a) 5×10^{15} ions/cm^2 at 40 keV, (b) 5×10^{15} ions/cm^2 at 80 keV, (c) 5×10^{15} ions/cm^2 at 150 keV, and (d) multirecipe of 5×10^{15} ions/cm^2, 1×10^{16} ions/cm^2, and 2×10^{16} ions/cm^2.

II. Experiment

SiO_2:Si^+ samples were prepared by multi-energy Si-ion implantation into a 5000-Å-thick SiO_2 film on 500-μm-thick, (100)-oriented, n-type Si substrate with a resistivity of 4–7 $\Omega \cdot$ cm. The SiO_2 film was deposited by PECVD under mixed tetraethoxysilane (TEOS) and O_2 with fluences of 10 and 200 sccm, respectively. The chamber pressure and power were 400 mTorr and 150 W, respectively. Si-implantation conditions were 5×10^{15} ions/cm^2 at 40 keV, 1×10^{16} ions/cm^2 at 80 keV, and 2×10^{16} ions/cm^2 at 150 keV. This results in a uniformly distributed Si-implantation profile with a depth of 100 and 5000 Å below the sample surface, as calculated by the simulation program, "transport of ions in matter" (TRIM) [5], as shown in Fig. 1. Some samples were encapsulated and annealed at 1100 °C in a quartz furnace tube under flowing

Manuscript received August 16, 2004; revised November 29, 2004. This work was supported in part by the National Science Council of the Republic of China under Grant NSC93-2215-E-009-007 and Grant NSC92-2215-E-009-028.

The authors are with the Department of Photonics and the Institute of Electro-Optical Engineering, National Chiao Tung University, Hsinchu, Taiwan 300, R.O.C. (e-mail: grlin@faculty.nctu.edu.tw).

Digital Object Identifier 10.1109/JQE.2004.842314

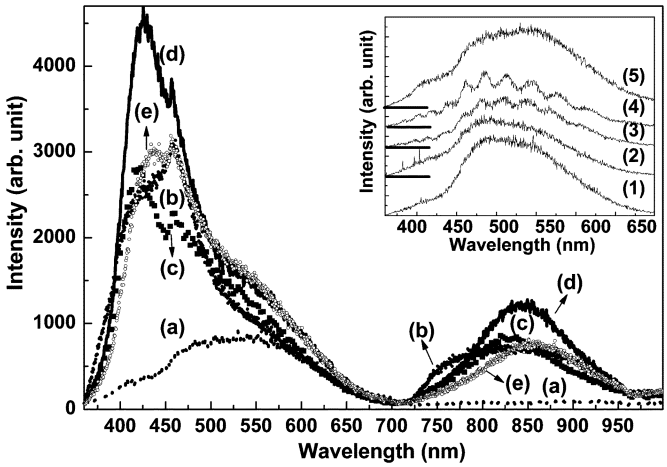

Fig. 2. PL spectra of the SiO_2:Si^+–Si samples at (a) as-implanted condition or annealed at 1100 °C for (b) 30, (c) 60, (d) 180 and (e) 240 min. The inset figure plots the PL spectra of (1) n-type Si substrate, (2) 60-min annealed n-type Si substrate, (3) SiO_2–Si sample, (4) 60-min annealed SiO_2–Si sample, and (5) as-implanted substrate.

N_2 gas for times ranging from 15 to 300 min, in order to help activate radiative defects and to eliminate the carrier-trapping centers buried in the SiO_2–Si substrate. To excite photoelectrons in the SiO_2:Si^+ sample for room-temperature and CW PL measurements, an He-Cd laser with a wavelength and an average intensity of 325 nm and 5 W/cm^2, respectively, were employed as the pumping source. The PL from 360 to 700 nm was resolved by a fluorescent spectrophotometer (Jobin Yvon, TRIAX-320) using a 1200-g/mm grating with a wavelength resolution of 0.06 nm and detected by a cooled photomultiplier (Jobin Yvon, Model 1424M)-based photon counter. The working distance between the focusing lens and the sample was fine-tuned to maximize the PL intensity. A MOS diode was made by coating 500-Å-thick 2-mm^2 silver contacts on the SiO_2:Si^+/n-Si substrate. After metallization, a sintering process was performed at 150 °C for 10 min in the ambient atmosphere. By using a pair of microprobes (Karr Suss, 253), the MOS diode was driven by either a pulsed current source (ILX, LDP-3840) or a voltage source meter (Keithley, 236). The pulsed current and the CW voltage were scanned from 0 V to 3 A and from 0 to 30 V, respectively. The optical power and bias voltage were measured using an optical multimeter (ILX, 6810B) and a digital multimeter (Hewlett Packard, HP34401A), respectively. An integrated-sphere detector (ILX, OMH-6703B) was employed to collect the light emitted from the MOS diode. The stability of the output power was measured at a pulsed current of 3 A for 3 h with a 10-ms period and a 10% duty cycle, respectively.

III. Results and Discussion

A. CW PL of SiO_2:Si^+

The inset in Fig. 2 presents the PL spectra of the Si substrate, the unimplanted SiO_2–Si, and the implanted SiO_2:Si^+–Si samples with and without annealing. As indicated by the inset in Fig. 2, the Si substrate exhibits a relatively weak and broadened PL spectrum between 500–550 nm, which becomes much weaker after annealing at 1100 °C for 60 min or longer. Similar results are observed for the unimplanted SiO_2–Si with an even weaker PL intensity before and after annealing at 1100 °C, revealing that very few radiative defects in the SiO_2–Si contribute to the green PL emission. In contrast, the peak PL intensity of the as-implanted SiO_2:Si^+ at 520 nm (in Fig. 2, line a) is equivalent to that of the Si substrate without annealing (Fig. 2 inset, line 1) and is much stronger than that of the SiO_2–Si (Fig. 2 inset, line 3). After annealing, a strong PL peak appears near 410–460 nm, as shown in Fig. 2 (lines b–e). The Si implantation introduces high concentrations of radiative defects into the SiO_2 film, which were thermally activated to enhance the blue–green PL spectrum at peak wavelengths of 415, 455, and 520 nm with linewidths of 35, 52, and 150 nm, respectively. The origin of these luminescent peaks has been reported [1], [8], [12], [13], but their evolution during long-term annealing has not been extensively addressed. The PL at 415 nm originates from the weak oxygen bond (WOB) defect [5] and the 455-nm luminescence is attributed to the NOV defect. The NBOHCs emit PL near 600 nm and the origin of the PL at 520 nm is associated with the E'_δ defect. The increase in PL intensity between 410–455 nm results mainly from the activation of radiative defects, including WOB and NOV defects in the SiO_2:Si^+ film. These structural defects are caused by the physical bombardment of the SiO_2 matrix under a multirecipe Si-implantation process. The strongest PL peaks at 415–455 nm with linewidths of 35–50 nm are very similar to those obtained by Nishikawa *et al.* [17], [18]. Bae *et al.* [19] have attributed the PL at 455 nm to the transition in the NOV defect [20], [21].

B. Defects in SiO_2:Si^+

During the Si implantation, the oxygen vacancies are created by the displacement of oxygen from a normal SiO_2 structure [15], and the oxygen interstitials (the precursors for the WOB defects) are generated concurrently. This process can be described by the reaction rule of $O_3 \equiv$ Si-O-Si $\equiv O_3 \rightarrow O_3 \equiv$ Si-Si $\equiv O_3 + O_{\text{interstitial}}$. Si implantation not only induces the strong displacement of the oxygen bonds, but also forms high concentrations of silicon/oxygen interstitials in the damaged lattice. Such oxygen interstitials have previously been reported in ion-implanted silica glass under various implantation conditions, including Si-implanted thermal SiO_2 ($2–3 \times 10^{17}$ cm^{-2}, 80–190 keV) [16], the Ge-implanted SiO_2 (5×10^{15} cm^{-2}, 80 keV) [19], and the Ir^{2+}-implanted silica glass ($0.6–7 \times 10^{16}$ cm^{-2}, 2 MeV) [18]. After annealing, the oxygen interstitials could also change into WOB defects by the reaction rule $O_{\text{interstitial}} + O_{\text{interstitial}} \rightarrow$ O–O. This reaction can be reversed under excessive thermal annealing energies, however, which explains the decrease in PL intensity from WOB defects in SiO_2:Si^+ samples that were annealed for more than 4 h.

EPR measurements were made to confirm the existence of E'_δ defects with a corresponding zero-crossing g value of approximately 2.0019 [22]–[25]. This EPR spectrum, in the inset of Fig. 3, reveals a complete activation of the E'_δ defects after annealing the SiO_2:Si^+ samples for 3 h [22], [23]. To verify the existence of NOV defects in SiO_2:Si^+, the absorption spectrum of the SiO_2:Si^+ layer was also measured. The resulting

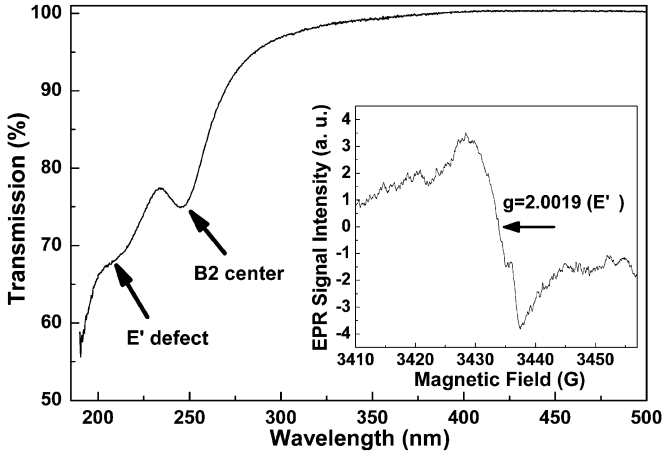

Fig. 3. Transmission spectrum of the SiO_2:Si^+ layer on a quartz layer after annealing for 90 min. The inset figure is the EPR spectrum of the 180-min-annealed SiO_2:Si^+.

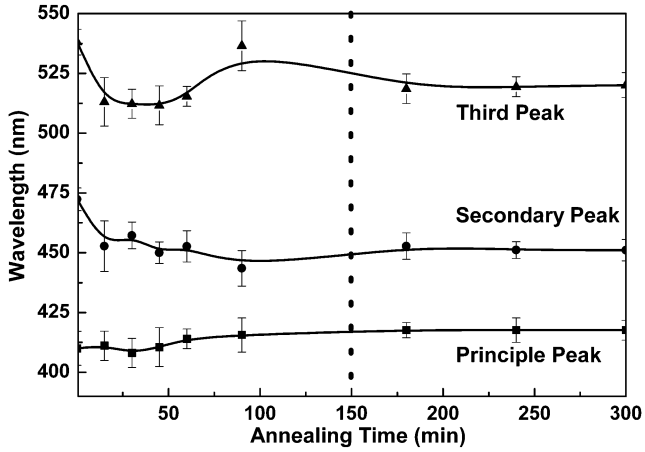

Fig. 4. Wavelength evolution of three PL peaks in SiO_2:Si^+ samples as-implanted or annealed at 1100 °C for different annealing times.

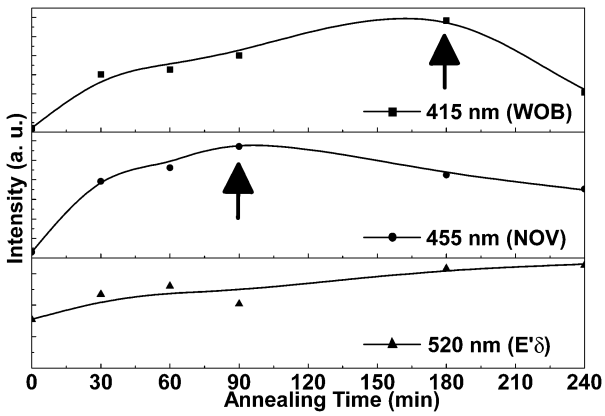

Fig. 5. Annealing-time-dependent PL intensities at different wavelengths of 415 nm (WOB defects), 455 nm (NOV defects), and 520 nm (E'_δ defects).

derivative absorption spectrum in Fig. 3 clearly indicates an absorption peak at 248 nm, which is attributed to the B_2 centers ($=$ Si:) reported elsewhere [26], [27]. Moreover, another absorption band related to the nonradiative E' defect ($O_3 \equiv Si \uparrow \cdot^+ Si \equiv O_3$) [26]–[28] is observed at 214 nm. A well-established model [29] shows that the optical absorption band at 5.8 eV (i.e., $\lambda =$ 214 nm) is related to the photo-ionization of the NOV defect [26]. Recently, Skuja *et al.* [30], [31] have proposed the divalent Si defects [$=$ Si: or a more neutral notation B_2(Si) center] as the candidate for the 5-eV absorption peak. They also performed time-resolved PL measurements of oxygen-deficient glassy SiO_2 and observed two luminescence bands at 4.4 eV (with a decay time of $<$ 4 ns) and 2.7 eV (with decay time of 10.2 ms). Based on their decay-time measurements, these two bands were individually attributed to the luminescence emission from the excited states of the B_2 centers and the neutral oxygen vacancy ($O_3 \equiv$ Si-Si $\equiv O_3$, NOV) defects, respectively.

The observation of both the 5-eV absorption peak (B_2 center dependent) and the 2.7-eV luminescence peak (NOV defect-dependent) in our samples provides evidence for the existence of both B_2 centers and NOV defects in the SiO_2:Si^+ materials. According to the results of Fig. 3, the intensity of the derivative absorption spectrum of the B_2 defect is much larger than that of the E' defect. In principle, both the intrinsic photo-ionization induced defect-formation mechanism and the extrinsic implantation-induced dissociation process can contribute to the formation of E' defects in SiO_2:Si^+ material. The intrinsic process involves the displacement of oxygen atoms from their positions in the perfect SiO_2 network through UV photon absorption and the subsequent generation of an E' center, as described by the reaction $O_3 \equiv$ Si-O-Si $\equiv O_3 \rightarrow O_3 \equiv Si \cdot^+ Si \equiv O_3 + O^-$. Such a process is relatively common under UV illumination conditions. On the other hand, the extrinsic process is a transformation of an NOV defect to an E' center, as described by the reaction $O_3 \equiv$ Si-Si $\equiv O_3 \rightarrow O_3 \equiv Si \cdot^+ Si \equiv O_3 + e^-$. Such a process cannot be ruled out since the WOB-related PL peak near 410 nm is also observed in the SiO_2:Si^+ sample, which confirms the generation of NOV defects and oxygen interstitials after the Si-ion-implantation-induced dissociation process, as described by $O_3 \equiv$ Si-O-Si $\equiv O_3 \rightarrow O_3 \equiv$ Si-Si $\equiv O_3 + O_{\text{interstitial}}$. At present, the experimental evidence reported here is insufficient to determine whether the dominant mechanism for generating E'_δ defects in SiO_2:Si^+ material is the intrinsic photo-ionization process or the extrinsic ion-implantation-induced dissociation process.

C. Evolution of Radiative Defects During the Annealing Duration

The results of the annealing-time-dependent PL wavelength and intensity indicate that the optimized annealing time at 1100 °C for stabilizing the PL wavelength is 3 h (see Figs. 4 and 5). The PL peak intensity increases abruptly during the first 15 min of annealing time, indicating that the elimination of nonradiative defects is more pronounced than the activation of radiative defects at this stage. The nonradiative defects are eliminated after annealing for 1 h or more. As the annealing time is increased, the activation of NOV defects becomes more pronounced than that of the WOB defects, leading to a slight red-shift of the PL from 415 to 455 nm. The radiative defects are completely activated after an annealing time of 1.5–3 h. After annealing for 3 h or more, the PL intensities at 415 and 455 nm decline considerably, whereas the PL intensity at 520 nm tends to remain constant or grows slightly stronger. It is thus believed that either the dominant radiative defects change from Si-O species (i.e., WOB and NOV defects) to E'_δ or NBOHC defects

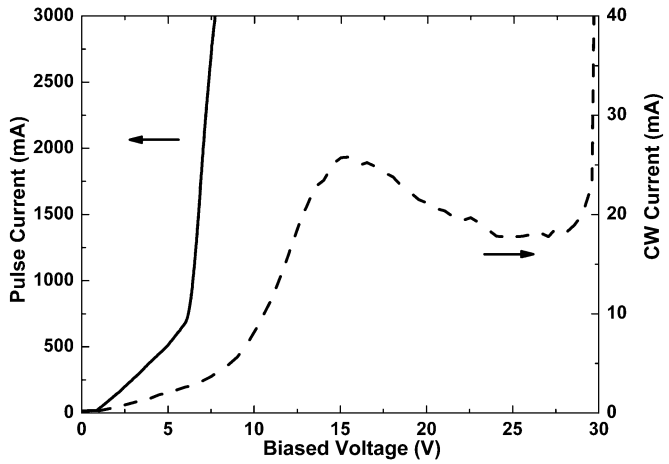

Fig. 6. CW and pulsed current–voltage measurements of Ag/SiO_2:Si^+/n-Si/Ag MOS diode with SiO_2:Si^+ annealing at 1100 °C for 180 min.

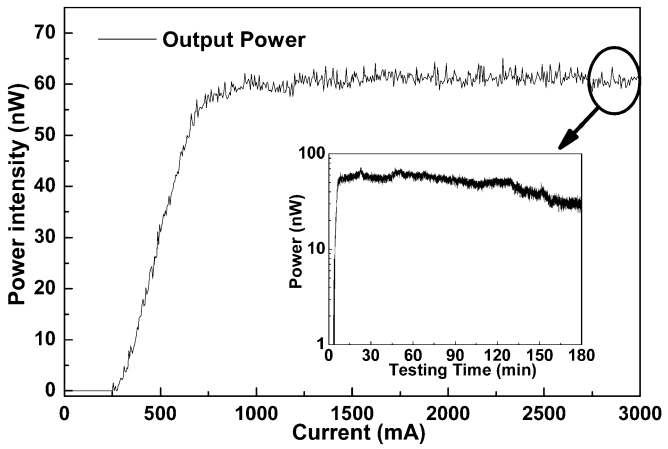

Fig. 7. Pulsed EL power as a function of the bias current. The inset figure is the lifetime and decaying rate of the Ag/SiO_2:Si/n-Si/Ag MOS diode under pulsed-current EL operation.

or they are annealed out faster than the E'_δ or NBOHC defects at a longer annealing time. Nonetheless, it should be noted that high-temperature annealing is expected to produce a complete recombination of point defects through the diffusion of mobile oxygen in SiO_2. On the other hand, such a high-temperature annealing condition (1100 °C for 15–180 min) has also been employed to precipitate Si nanocrystals in a similar material system [6], [7], [10]. The excess Si atoms segregate from the SiOx matrix under high-temperature conditions and precipitate one another to form Si nanocrystals. Shimizu-Iwayama *et al.* [7] have observed a strong luminescence peak at 1.7 eV from high-energy (1 MeV) Si^+-implanted silica with an implantation dose of 1×10^{17} ions/cm^2 after thermal annealing at 1100 °C for 1 h. In the high-dose ($0.3–3 \times 10^{17}$ ions/cm^2) Si^+-implanted SiO_2 layer grown on silicon substrates, Mutti *et al.* [6] observed both a visible luminescence from the as-implanted sample and a broad-band near-infrared luminescence centered beyond 750 nm from the annealed sample. In contrast, the near-infrared PL spectra from our low-dose-implanted SiO_2:Si^+–Si samples in Fig. 2 are still weak, even after annealing times as long as 4 h. Indeed, a red-shifted PL is observed from 826 to 856.5 nm in Fig. 2, which corroborates the increasing size of Si nanocrystals after annealing from 1 to 4 h. The maximum PL intensity is also obtained in the 3-h annealed sample. Nonetheless, the intensities of the nc-Si-related near-infrared PL peaks (826–856 nm) are much smaller than those contributed by the radiative defects, including the WOB (415 nm), NOV (455 nm), and E'_δ (520 nm) defects. These results suggest that the low-dose implantation process used here provides a low excess Si contribution ($<3\%$) in the SiO_2 matrix, thus providing insufficient nc-Si precursors and resulting in a very low density of nc-Si precipitates embedded in the SiO_2 matrix after annealing. This low excess Si concentration may thus explain why the blue–green emission dominates over the near-infrared emission in our samples, even after annealing times as long as 4 h.

D. Electroluminescence of Ag/SiO_2:Si^+/n-Si/Ag MOS Diode

Fig. 6 presents the measured CW and pulsed current–voltage (I–V) characteristics of the Ag/SiO_2:Si^+/n-Si/Ag MOS diode. The turn-on voltage of the MOS diode under the pulsed driving condition is 5.8 V, which is much smaller than that of the Ag/SiO_2/n-Si/Al MOS diode reported previously [32]. The CW I–V measurements of the Ag/SiO_2:Si^+/n-Si/Ag MOS diode further reveal a negative-differential-resistance effect with a threshold field strength (300 kV/cm) comparable to that of the GaN semiconductors (80-150 kV/cm) [33], [34]. The resistance of the Ag/SiO_2:Si^+/n-Si/Ag MOS diode is about 7.9 Ω at a bias voltage between 0–9 V, but the resistance decreases to 0.6 Ω after turn-on. Significantly, the turn-on voltage of the Ag/SiO_2:Si^+/n-Si/Ag MOS diode is almost one order of magnitude lower than that of an Ag/SiO_2/n-Si/Al diode (up to 50 V) reported by Yuan *et al.* [32]. Under pulsed current driving conditions, the optical power of the SiO_2:Si^+ MOS diode driven from 0 to 3 A is shown in Fig. 7. Extrapolating the output optical power as a function of the bias current or voltage reveals that the threshold current of the Ag/SiO_2:Si^+/n-Si/Ag MOS light-emitting diode is 0.28 A. Such a low turn-on voltage of the emission of light from the Ag/SiO_2:Si^+/n-Si/Ag MOS diode SiO_2:Si^+ sample with a SiO_2:Si^+ thickness of 500 nm is mainly attributed to the improvement (modification) of the carrier transport of the Ag/SiO_2:Si^+/Si/Ag MOS diode, which is strongly related to the enhanced Fowler–Nordheim tunneling behavior induced after the multi-energy Si-implantation process. The optical power increases by nearly four orders of magnitude as the drive current is increased from 0.28 to 0.97 A. The maximum optical power is about 120 nW at a bias current of 0.97 A. By measuring a single luminescent point of the Ag/SiO_2:Si^+/n-Si/Ag diode with a lensed fiber, the power–current (P–I) slope is determined as to be 1.56×10^{-5} mW/A. Note that such a small slope is due to the measuring limit of the power sensor. The optical power at a constant drive current is relatively stable, with a fluctuation of less than 5%. As the drive current exceeds 1 A, the output power tends to saturate due to the finite density of minority carrier (holes) in n-Si injected into the SiO_2:Si^+ layer (see Fig. 7).

The EL wavelength of the Ag/SiO_2:Si^+/n-Si/Ag MOS diode is completely different from that of an Ag/SiO_2/n-Si/Al diode (with red luminescence at wavelengths of 620-640 nm) [10]. In particular, the far-field EL patterns of the Ag/SiO_2:Si^+/n-Si/Ag

Fig. 8. Far-field EL patterns at different bias currents of (a) 0.35, (b) 1.25, and (c) 3 A.

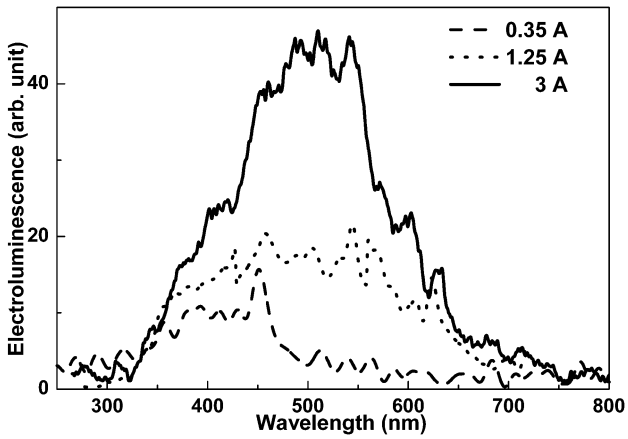

Fig. 9. EL spectra of the Ag/SiO_2:Si^+/n-Si/Ag MOS diode at different bias currents of 0.35 (dashed line), 1.25 (dotted line), and 3 A (solid line).

MOS diode biased at various pulsed currents (see Fig. 8) reveal different colors under different bias conditions. The deep-blue EL is more pronounced at a bias current near threshold, which turns into the white-light luminescence at a bias current of 1.25 A. However, the dominant EL wavelength further increases into the green region as the bias current becomes extremely high (>2 A). At a bias current of 0.35 A, the deep-blue EL spectrum (see Fig. 9) of the MOS diode is between 400–450 nm since the recombination by WOB defects is preferable under near-threshold conditions. The white-light EL spectrum of the MOS diode at a bias current of 1.25 A is between 400–600 nm, while the green EL spectrum at 3 A is between 450–550 nm. At a bias current of 1.25 A, the white-light emission is attributed to a full recombination through three different centers, including the WOB defects (∼415 nm), the NOV defects, and the E'_δ defects (∼520 nm). At a high bias current (>2 A), the green-region spectrum is clearly enhanced due to the highest density of NOV defects in SiO_2:Si^+. The EL intensity at a bias current of 3 A is six times higher than that at 0.35 A. Additionally, the emission spot becomes larger at a higher bias. The lifetime testing of such an EL emitting diode is performed by measuring its time-dependent power characteristic, as shown in the inset of Fig. 7. Under a pulsed bias of 3 A, the decay in output power of the Ag/SiO_2:Si^+/n-Si/Ag MOS diode under TEC cooling is up to 58% within 3 h.

E. Electroluminescent Mechanism of SiO_2:Si^+

The EL spectrum of the Ag/SiO_2:Si^+/n-Si/Ag MOS diode deviates slightly from that of the PL, which originates from an impact ionization and subsequent electron–hole recombination under a high electric field. Previously, Heikkilä *et al.* [35] have studied versatile carrier transport mechanisms of the metal/SiO_2/p-Si/metal diode. The light emission from such a MOS diode is mainly dependent on the defects near the interface of the SiO_2/p-Si, which exhibits EL under both the forward and reverse bias conditions only when the contact metal is ohmic-like. The schematic energy-band diagrams of the metal/SiO_2/p-Si/metal structure under forward and reverse bias are shown in previous work [19], [32], [35]. If a forward bias is sufficiently large, most electrons from the negatively biased metal contact can tunnel through the SiO_2 into the conduction band of p-Si substrate, and some electrons can be trapped by the higher energy levels of the defects in the SiO_2 [19], [35]. The holes (majority carriers) in p-Si can also be injected into the SiO_2 and be trapped by higher energy levels of the defects in the SiO_2. The radiative recombination of charged carriers at these occupied defect states in the SiO_2 is responsible for the visible EL. When the metal/SiO_2/p-Si/metal diode is negatively biased, the holes can hardly be supported by the metal contact, and the electrons are the minority carriers in p-Si. Consequently, a strong EL is rather difficult unless the MOS diode is strongly reverse-biased.

In addition, Yuan *et al.* [32] also observed a visible EL at 620–640 nm from a reverse-biased Ag/native-SiO_2/n-Si/Al (referred to as Ag/SiO_2/n-Si/Al) diode, which results from the recombination of NBOHC centers near the SiO_2/n-Si interface. The carrier injection of such a diode structure relies on the field-dependent impact ionization [19], [32], [35]. Under a reverse bias, an inversion layer can be formed just beneath the SiO_2/n-Si interface, which accumulates the minority carriers (holes) in n-Si as shown in [32, Fig. 5(b)]. The tunneling electrons from the metal contact and holes from the n-Si are subsequently trapped and radiatively recombine through the NBOHC states. In particular, a forward bias fails to induce EL since it is difficult to inject holes from the positively biased metal contact. These observations correlate well with previous reports where the metal contact must supply electrons rather than holes. Such polarization dependence also excludes the possibility of EL from nc-Si (if it exists) within the SiO_2. Later on, Bae *et al.* [19] stated that the EL observed in an Au/SiO_x/p-Si/metal diode under reverse bias is attributed to the impact ionization of the ground-state electrons of the NOV centers in SiO_x. It is considered that luminescent efficiency by direct tunneling under a forward bias is less pronounced than that by impact ionization under reverse bias, although the direct tunneling helps the transport of carriers under forward bias conditions.

In comparison, our experimental results are somewhat similar to those reported previously [10], [22], which reveals that the EL of the Si-rich SiO_2:Si^+ layer decreases under forward-bias conditions [19], [36], [37]. The EL can only be obtained when the Ag–SiO_2:Si^+/n-Si–Ag diode is reverse biased in our case, which is enhanced by stronger impact ionization on the ground states of defects via the accumulation of injected holes in the inversion layer formed beneath the SiO_2:Si^+/n-Si interface. In general, multi-energy Si-ion implantation introduces high densities of various defects that are uniformly distributed in the thin SiO_2:Si^+ layer. With increasing bias, the tunneling electrons and holes can be trapped and subsequently recombine in the occupied WOB defect, NOV defects, and E'_δ defects. A higher electric field increases the band bending in the accumulation

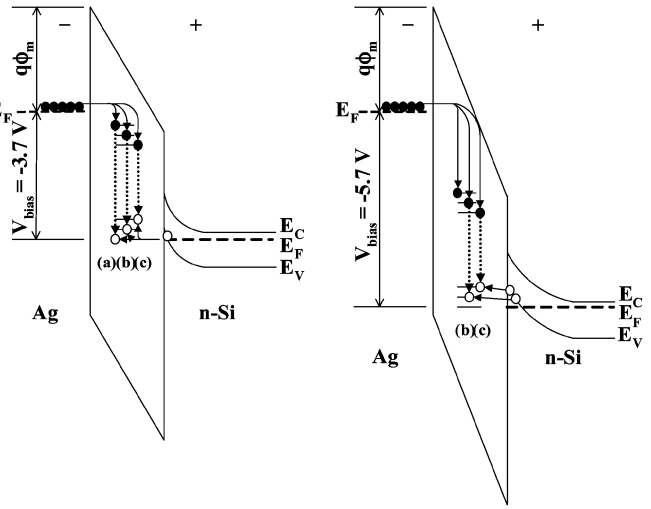

Fig. 10. Energy-band diagrams of the Ag/SiO_2:Si^+/n-Si/Ag structure with metal–oxide barrier potential of $\phi_m = 3.28$ V under reverse bias at 3.7 V (left) and 5.7 V (right). Three defect-related radiative emissions at (a) 415 nm from the WOB defect, (b) 455 nm from the NOV defect, and (c) 520 nm from the E'_δ defect.

layer, which facilitates the tunneling of holes from the n-Si substrate to the ground states of NOV and E'_δ defects (see Fig. 10). Such an operation greatly enhances the transitions contributing to the blue–yellow luminescence. Both of the transitions contributed by the WOB defects and NOV defects can emit the deep-blue luminescence at lower bias currents. The white-light EL emission is observed when the bias current increases before the saturation of output power. The green EL from the E'_δ will be enhanced when the bias current (as well as the electric field) becomes extremely high. The reason for the saturated output power at a bias current of nearly 1 A is due to the limited density of the minority carriers (holes) in the n-Si substrate. A stronger bias seriously bends the inversion layer beneath the SiO_2:Si^+/n-Si interface and thus greatly accumulates the holes at lower states, which subsequently tunnel into the E'_δ defects at higher energy levels (see Fig. 10). This effect results in longer luminescent wavelengths at higher bias conditions. Nonetheless, such an impact ionization process usually requires a strong bias, which inevitably causes the substrate to overheat.

IV. Conclusion

The white-light and blue–green EL from an Ag/SiO_2:Si^+/n-Si/Ag MOS diode with the defect-enhanced blue–green PL, made on a thermally annealed multirecipe Si-ion-implanted SiO_2:Si^+ film on an Si substrate with a nearly depth-independent Si-dose distribution profile, are studied. After annealing for 180 min, the main radiative defects corresponding to PL at 415, 455, and 520 nm are completely activated. These defects are identified as WOB, the NOV-related defects, and E'_δ-related defects, respectively. Ion implantation introduces more dangling bond defects than other methods (such as PECVD and sputtering) for synthesizing the Si-rich SiO_2. During the Si implantation (or physical bombardment with high-energy ions), the oxygen vacancies and the oxygen interstitials (the precursors for the WOB defects) are created due to the relatively large quantities of oxygen that are displaced from their atomic positions in the SiO_2 matrix. In comparison with NOV defects, additional energy is required to form WOB defects from the oxygen interstitials. The NOV defects are therefore activated faster than the WOB defects for a given annealing condition, however, the increase in the number of both NOV and WOB radiative defects are of the same order of magnitude. This result again confirms the reaction rule for oxygen vacancies and interstitials in SiO_2:Si^+. The reduction in the density of the WOB defects is more pronounced than that of NOV defects since two oxygen interstitials are required to generate a WOB defect. The complete activation of the E'_δ defects does not happen in experimental results, which reveals the nc-Si structures have not yet been well constructed. The EL power of the Ag/SiO_2:Si^+/n-Si/Ag MOS diode increases linearly with bias current after turn-on and saturates near 0.97 A. The EL of the Ag/SiO_2:Si^+/n-Si/Ag MOS diode turns from blue to white-light emission when the bias current is close to the saturation condition and eventually changes to a yellow–green emission as the bias current is increased to 3 A. The EL spectrum of the MOS diode under different reverse-bias conditions indicates that the radiative recombination is due to enhanced impact ionization of ground states of defects, such as WOB, NOV, and E'_δ defects, through the injection of holes accumulated in the inversion layer formed beneath the SiO_2:Si^+/n-Si interface.

Acknowledgment

The authors would like to thank Dr. J.-M. Shieh, National Nano Device Laboratory, for his technical support.

References

[1] Q. Ye, R. Tsu, and E. H. Nicollian, "Resonant tunneling via microcrystalline-silicon quantum confinement," *Phys. Rev. B, Condens. Matter*, vol. 44, no. 4, pp. 1806–1811, July 1991.

[2] A. Pèrez-Rodrìguez, O. González-Varona, B. Garrido, P. Pellegrino, J. R. Morante, C. Bonafos, M. Carrada, and A. Claverie, "White luminescence from Si^+ and C^+ ion-implanted SiO_2 films," *J. Appl. Phys.*, vol. 94, no. 1, pp. 254–261, Jul. 2003.

[3] D. Pacifici, E. C. Moreira, G. Franzo, V. Martorino, and F. Priolo, "Defect production and annealing in ion-irradiated Si nanocrystals," *Phys. Rev. B, Condens. Matter*, vol. 65, no. 14, pp. 144 109-1–144 109-13, Apr. 2002.

[4] L. T. Canham, "Silicon quantum wire array fabrication by electrochemical and chemical dissolution of wafers," *Appl. Phys. Lett.*, vol. 57, no. 10, pp. 1046–1048, Sep. 1990.

[5] X. Zhao, O. Schoenfeld, J. Kusano, Y. Aoyagi, and T. Sugano, "Observation of direct transitions in silicon nanocrystallites," *Jpn. J. Appl. Phys.*, vol. 33, no. 7A, pp. L899–L901, Jul. 1994.

[6] P. Mutti, G. Ghislotti, S. Bertoni, L. Bonoldi, G. F. Cerofolini, L. Meda, E. Grilli, and M. Guzzi, "Room-temperature visible luminescence from silicon nanocrystals in silicon implanted SiO_2 layers," *Appl. Phys. Lett.*, vol. 66, no. 7, pp. 851–853, Feb. 1995.

[7] T. Shimizu-Iwayama, K. Fujita, S. Nakao, K. Saitoh, T. Fujita, and N. Itoh, "Visible photoluminescence in Si^+ -implanted silica glass," *J. Appl. Phys.*, vol. 75, no. 12, pp. 7779–7783, Jun. 1994.

[8] H. Takagi, H. Owada, Y. Yamazaki, A. Ishizaki, and T. Nakagiri, "Quantum size effects on photoluminescence in ultrafine Si particles," *Appl. Phys. Lett.*, vol. 56, no. 24, pp. 2379–2380, Jun. 1990.

[9] S. Tong, X. N. Liu, T. Gao, and X. M. Bao, "Intense violet-blue photoluminescence in as-deposited amorphous Si:H:O films," *Appl. Phys. Lett.*, vol. 71, no. 5, pp. 698–700, Aug. 1997.

[10] L. S. Liao, X. M. Bao, X. Q. Zheng, N. S. Li, and N. B. Min, "Blue luminescence from Si^+ -implanted SiO_2 films thermally grown on crystalline silicon," *Appl. Phys. Lett.*, vol. 68, no. 6, pp. 850–852, Feb. 1996.

[11] H. Z. Song, X. M. Bao, N. S. Li, and J. Y. Zhang, "Relation between electroluminescence and photoluminescence of Si^+-implanted SiO_2," *J. Appl. Phys.*, vol. 82, no. 8, pp. 4028–4032, Oct. 1997.
[12] G. G. Qin, A. P. Li, B. R. Zhang, and B. C. Li, "Visible electroluminescence from semitransparent au film/extra thin Si-rich silicon oxide film/p-Si structure," *J. Appl. Phys.*, vol. 78, no. 3, pp. 2006–2009, Aug. 1995.
[13] H. Z. Song and X. M. Bao, "Visible photoluminescence from silicon-ion-implanted SiO_2 film and its multiple mechanisms," *Phys. Rev. B, Condens. Matter*, vol. 55, no. 11, pp. 6988–6993, Mar. 1997.
[14] W. Hayes, M. J. Kane, O. Salminen, R. L. Wood, and S. P. Doherty, "ODMR of recombination centers in crystalline quartz," *J. Phys. C: Solid State Phys.*, vol. 17, pp. 2943–2951, Dec. 1984.
[15] H. Nishikawa, E. Watanabe, D. Ito, M. Takiyama, A. Leki, and Y. Ohki, "Photoluminescence study of defects in ion-implanted thermal SiO_2 films," *J. Appl. Phys.*, vol. 78, no. 2, pp. 842–846, Jul. 1995.
[16] R. Tohmon, Y. Shimogaichi, H. Mizuno, Y. Ohki, K. Nagasawa, and Y. Hama, "2.7-eV luminescence in as-manufactured high-purity silica glass," *Phys. Rev. Lett.*, vol. 62, no. 2, pp. 1388–1391, Mar. 1989.
[17] H. Nishikawa, R. E. Stahlbush, and J. H. Stathis, "Oxygen-deficient centers and excess Si in buried oxide using photoluminescence spectroscopy," *Phys. Rev. B, Condens. Matter*, vol. 60, no. 23, pp. 15 910–15 918, Dec. 1999.
[18] J. C. Cheang-Wong, A. Oliver, J. Roiz, J. M. Hernandez, L. Rodrigues-Fernandez, J. G. Morales, and A. Crespo-Sosa, "Optical properties of Ir^{2+}-implanted silica glass," *Nucl. Instr. Meth. B*, vol. 175–177, pp. 490–494, Apr. 2001.
[19] H. S. Bae, T. G. Kim, C. N. Whang, S. Im, J. S. Yun, and J. H. Song, "Electroluminescence mechanism in SiO_x layers containing radiative centers," *J. Appl. Phys.*, vol. 91, no. 7, pp. 4078–4081, Apr. 2002.
[20] E. H. Poindexter and P. J. Caplan, "Electron spin resonance of inherent and process induced defects near the Si/SiO_2 interface of oxidized silicon wafers," *J. Vac. Sci. Technol. A*, vol. 6, no. 3, pp. 1352–1357, May 1988.
[21] B. L. Zhang and K. Raghavachari, "Photoabsorption and photoluminescence of divalent defects in silicate and germanosilicate glasses: First-principles calculations," *Phys. Rev. B, Condens. Matter*, vol. 55, no. 24, pp. R15993–R15996, June 1997.
[22] K. Vanheusden and A. Stesmans, "Characterization and depth profiling of E' defects in buried SiO_2," *J. Appl. Phys.*, vol. 74, no. 1, pp. 275–283, Jul. 1993.
[23] Y. Sakurai and K. Nagasawa, "Green photoluminescence band in γ-irradiated oxygen-surplus silica glass," *J. Appl. Phys.*, vol. 86, no. 3, pp. 1377–1381, Aug. 1999.
[24] H. Nishikawa, E. Watanabe, D. Ito, Y. Sakurai, K. Nagasawa, and Y. Ohki, "Visible photoluminescence from Si clusters in γ-irradiated amorphous SiO_2," *J. Appl. Phys.*, vol. 80, no. 6, pp. 3513–3517, Sep. 1996.
[25] M. Y. Valakh, V. A. Yukhimchuk, V. Y. Bratus, A. A. Konchits, P. L. F. Hemment, and T. Komoda, "Optical and electron paramagnetic resonance study of light-emitting Si^+ ion implanted silicon dioxide layers," *J. Appl. Phys.*, vol. 85, no. 1, pp. 168–173, Jan. 1999.
[26] B. L. Zhang and K. Raghavachari, "Photoabsorption and photoluminescence of divalent defects in silicate and germanosilicate glasses: First-principles calculations," *Phys. Rev. B, Condens. Matter*, vol. 55, no. 24, pp. R15993–R15996, June 1997.
[27] C. Barthou, P. H. Duong, A. Oliver, J. C. Cheang-Wong, L. Rodríguez-Fernández, A. Crespo-Sosa, T. Itoh, and P. Lavallard, "Silicon nanocrystals and defects produced by silicon and silicon-and-gold implantation in silica," *J. Appl. Phys.*, vol. 93, no. 12, pp. 10 110–10 113, Jun. 2003.
[28] A. Anedda, R. Boscaino, M. Cannas, R. Corpino, F. M. Gelardi, and M. Leone, "Experimental evidence of the composite nature of the 3.1 eV luminescence in natural silica," *Nucl. Instrum. Methods Phys. Res. B*, vol. 116, no. 1–4, pp. 360–363, Aug. 1996.
[29] R. A. Weeks and E. Sonder, *Paramagnetic Resonance*. New York: Academic, 1963, pp. 869–869.
[30] L. Skuja, "Direct singlet-to-triplet optical absorption and luminescence excitation band of the twofold-coordinated silicon center in oxygen-deficient glassy SiO_2," *J. Non-Cryst. Solids*, vol. 167, no. 3, pp. 229–238, Feb. 1994.
[31] ——, "Optically active oxygen-deficiency-related centers in amorphous silicon dioxide," *J. Non-Cryst. Solids*, vol. 239, no. 1–3, pp. 16–48, Oct. 1998.
[32] J. Yuan and D. Haneman, "Visible electroluminescence from native SiO_2 on n-type Si substrates," *J. Appl. Phys.*, vol. 86, no. 4, pp. 2358–2360, Aug. 1999.
[33] G.-R. Lin, "The structural and electrical characteristics of silicon-implanted borosilicate glass," *Jpn. J. Appl. Phys.*, vol. 41, no. 12A, pp. L1379–L1382, Dec. 2002.
[34] E. Alekseer and D. Pavlidis, "Large-signal microwave performance of GaN-based NDR diode oscillators," *Solid-State Electron.*, vol. 44, no. 6, pp. 941–947, Jun. 2000.
[35] L. Heikkilä, T. Kuusela, and H.-P. Hedman, "Electroluminescence in Si/SiO_2 layer structures," *J. Appl. Phys.*, vol. 89, no. 4, pp. 2179–2184, Feb. 2001.
[36] M. Kimura and H. Koyama, "Mechanism of time-dependent oxide breakdown in thin thermally grown SiO_2 films," *J. Appl. Phys.*, vol. 85, no. 11, pp. 7671–7681, Jun. 1999.
[37] H. J. Wen and R. Ludeke, "Investigation of existing defects and defect generation in device-grade SiO_2 by ballistic electron emission spectroscopy," *J. Vac. Sci. Technol. B*, vol. 15, no. 4, pp. 1080–1088, Jul. 1997.

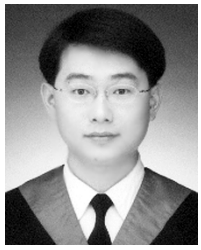

Chun-Jung Lin was born in Taipei, Taiwan, R.O.C., in 1973. He received the B.S. degree in electrical engineering from Feng Chia University, Taichung, Taiwan, in 1998 and the M.S. degree in electrooptic engineering from Tatung University, Taipei, in 2000. He is currently working toward the Ph.D. degree in electrooptic engineering at the National Chiao Tung University, Hsinchu, Taiwan.

From 2001 to 2002, he was with Kingfont Inc., Taipei, as a Senior Engineer, where he was involved with fiber transceivers. His research interests are in the design, fabrication, and analysis of nanocrystal photonic components for light-emitting devices.

Gong-Ru Lin (S'92–M'97–SM'04) received the M.S. and Ph.D. degrees from National Chiao Tung University (NCTU), Hsinchu, Taiwan, R.O.C., in 1990 and 1996, respectively.

He joined NCTU as an Associate Professor with the Institute of Electro-Optical Engineering in 2002. His research interests are in ultrafast fiber lasers and optoelectronics, microwave and millimeter-wave photonics, and amorphous or nanocrystallite semiconductors. He has (co)authored more than 70 papers in international periodicals and over 100 papers in international conferences.

Dr. Lin is currently a Senior Member of the IEEE Lasers and Electro-Optics and Microwave Theory and Techniques Societies and a member of the Optical Society of America and SPIE. He has been included in *Who's Who in Science and Engineering*, (6th ed.) since 2002. He was the recipient of the Tien Jea Bien Young Scholar Prize by the Optical Engineering Society of the Republic of China for his outstanding achievement in photonics.